

RESEARCH PAPER

A novel plasminogen activator inhibitor-1 inhibitor, TM5441, protects against high-fat diet-induced obesity and adipocyte injury in mice

Correspondence Professor Hunjoo Ha, Graduate School of Pharmaceutical Sciences, College of Pharmacy, Ewha Womans University, 52, Ewhayeodae-gil, Seodaemun-gu, Seoul 120-750, Korea. E-mail: hha@ewha.ac.kr

Received 28 January 2016; **Revised** 11 June 2016; **Accepted** 16 June 2016

Lingjuan Piao^{1*}, Inji Jung^{1*}, Joo Young Huh², Toshio Miyata³ and Hunjoo Ha¹

¹Graduate School of Pharmaceutical Sciences, College of Pharmacy, Ewha Womans University, Seoul, Korea, ²Colleges of Pharmacy, Chonnam National University, Gwang-Ju, Korea, and ³United Centers for Advanced Research and Translational Medicine, Tohoku University Graduate School of Medicine, Sendai, Japan

*Lingjuan Piao and Inji Jung contributed equally to this study.

BACKGROUND AND PURPOSE

Obesity is one of the most prevalent chronic diseases worldwide, and dysregulated adipocyte function plays an important role in obesity-associated metabolic disorder. The level of plasma plasminogen activator inhibitor-1 (PAI-1) is increased in obese subjects, and PAI-1 null mice show improved insulin sensitivity when subjected to high-fat and high-sucrose diet-induced metabolic stress, suggesting that a best-in-class PAI-1 inhibitor may become a novel therapeutic agent for obesity-associated metabolic syndrome. TM5441 is a novel orally active PAI-1 inhibitor that does not cause bleeding episodes. Hence, in the present study we examined the preventive effect of TM5441 on high-fat diet (HFD)-induced adipocyte dysfunction.

EXPERIMENTAL APPROACH

Ten-week-old C57BL/6J mice were fed a normal diet (18% of total calories from fat) or HFD (60% of total calories from fat) for 10 weeks, and TM5441 (20 mg·kg⁻¹ oral gavage) was administered daily with the initiation of HFD.

KEY RESULTS

TM5441 prevented HFD-induced body weight gain and systemic insulin resistance. TM5441 normalized HFD-induced dysregulated JNK and Akt phosphorylation, suggesting that it prevents the insulin resistance of adipocytes. TM5441 also attenuated the macrophage infiltration and increased expression of pro-inflammatory cytokines, such as inducible nitric oxide synthase, induced by the HFD. In addition, TM5441 prevented the HFD-induced down-regulation of genes involved in mitochondrial biogenesis and function, suggesting that it may prevent adipocyte inflammation and dysregulation by maintaining mitochondrial fitness.

CONCLUSION AND IMPLICATIONS

Our data suggest that TM5441 may become a novel therapeutic agent for obesity and obesity-related metabolic disorders.

Abbreviations

ATGL, adipose triglyceride lipase; Cox, cytochrome c oxidase; FAS, fatty acid synthase; FFA, free fatty acid; GTT, glucose tolerance test; H&E, haematoxylin and eosin; HFD, high-fat diet; HSL, hormone-sensitive lipase; iNOS, inducible nitric oxide synthase; ITT, insulin tolerance test; KO, knockout; MCP-1, monocyte chemoattractant protein-1; mtDNA, mitochondrial DNA; ND, normal diet; PAI-1, plasminogen activator inhibitor-1; PGC1 α , PPAR γ coactivator-1 α ; Tfam, mitochondrial transcription factor A; TG, triglyceride; TM5275, 5-chloro-2-[[2-[4-(diphenylmethyl)piperazin-1-yl]-2-oxoethoxy]acetyl]amino]benzoate; TM5441, 5-chloro-2-[[2-[[3-(furan-3-yl)phenyl]amino]-2-oxoethoxy]acetyl]amino] benzoic acid; UCP, uncoupling protein; WAT, white adipose tissue

Tables of Links

TARGETS	
Enzymes ^a	Transporters ^b
Akt (PKB)	UCP-1
FASN	
Hormone sensitive lipase (HSL)	
iNOS	
JNK	

LIGANDS
Cholesterol
Glycerol
Insulin
MCP-1 (CCL2)

These Tables list key protein targets and ligands in this article which are hyperlinked to corresponding entries in <http://www.guidetopharmacology.org>, the common portal for data from the IUPHAR/BPS Guide to PHARMACOLOGY (Southan *et al.*, 2016) and are permanently archived in the Concise Guide to PHARMACOLOGY 2015/16 (^{a,b}Alexander *et al.*, 2015a,b).

Introduction

Obesity, a condition of abnormal or excessive fat accumulation in adipose tissue, is increasing to epidemic proportions worldwide (Smyth and Heron, 2006). Because obesity leads to detrimental metabolic effects such as coronary heart disease, ischaemic stroke and type 2 diabetes mellitus (Hotamisligil, 2006), a novel effective anti-obesity agent is a therapeutic goal. Obesity and obesity-related metabolic disorders inflict a variety of stresses on adipose tissues, including hypertrophy, inflammation and metabolic load. During obesity, adipose tissue not only becomes resistant to the effects of insulin but also plays a critical role in regulating whole body insulin resistance through altered secretion of adipokines, which act in an autocrine, paracrine and endocrine manner (Rudich *et al.*, 2007).

Plasminogen activator inhibitor-1 (PAI-1), a glycoprotein with a molecular weight of 50 kDa that belongs to a family of serine protease inhibitors, is an endogenous inhibitor of tissue-type or urokinase-type plasminogen activators and blocks fibrinolysis. Increased circulating PAI-1 has been associated with not only thrombosis and fibrosis but also insulin resistance (Juhan-Vague *et al.*, 1991; Mertens *et al.*, 2006). Mice lacking functional PAI-1 are protected from obesity and insulin resistance (Ma *et al.*, 2004). Also, primary adipocytes from PAI-1 knockout (KO) mice exhibit improved basal as well as insulin-stimulated glucose uptake compared with those from wild type mice (Ma *et al.*, 2004). These findings suggest that PAI-1 is involved in the regulation of fat accumulation and that PAI-1 inhibition has potential clinical benefits as a new therapeutic target for treating obesity by reducing body weight and improving insulin sensitivity. In fact, pharmacological inhibition of PAI-1 (PAI-039) for 4 weeks improved high-fat diet (HFD)-induced obesity and circulating plasma active PAI-1 (Crandall *et al.*, 2006). PAI-039, however, has not been developed further clinically because of its lack of activity against vitronectin-bound PAI-1 (Gorlatova *et al.*, 2007). Based on the three-dimensional structure of PAI-1, a novel orally active PAI-1 inhibitor, TM5275, has been developed (Izuhara *et al.*, 2010). Furthermore, TM5441, a derivative of TM5275 with an improved pharmacokinetic profile, has been reported to have beneficial effects in various conditions. TM5441 attenuates N^o-nitro-L-arginine methyl ester-induced cardiac hypertension and

vascular senescence (Boe *et al.*, 2013), prolongs lifespan in klotho null mice (Eren *et al.*, 2014) and elicits anti-tumorigenic and anti-angiogenic activities in cancer (Placencio *et al.*, 2015). The effect of TM5441 on obesity *in vivo* has not yet been explored.

While the exact mechanism involved in PAI-1-induced insulin resistance is still elusive, mitochondrial dysfunction has been proposed to play an important role in the development of obesity and metabolic disorder (Patti and Corvera, 2010). A recent report showing that adipose-specific *crif1* deficiency reduces mitochondrial oxidative phosphorylation and obesity (Ryu *et al.*, 2013) supports the notion that mitochondrial dysfunction may trigger inflammation and insulin resistance. We have previously demonstrated that an impaired mitochondrial antioxidant system in peroxiredoxin 3 deficiency leads to an increase in adipose PAI-1 levels and insulin resistance (Huh *et al.*, 2012). We, therefore, hypothesized that TM5441 ameliorates dysregulated metabolism in adipocytes and investigated whether this orally active novel PAI-1 inhibitor can prevent obesity and adipocyte injury in diet-induced obese mice. The present study further examined the pharmacological mechanism of the effects of TM5441 on dysregulated metabolism in adipocytes focusing on mitochondrial fitness.

Methods

Animals

Animal studies are reported in compliance with the ARRIVE guidelines (Kilkenny *et al.*, 2010; McGrath and Lilley, 2015). Ten-week-old C57BL/6J mice were housed in a room maintained at 22 ± 2°C with a 12 h dark/12 h light cycle and fed either a normal diet (ND) or an HFD (containing 18.4% protein-derived calories, 21.3% carbohydrate-derived calories and 60% fat-derived calories, Harlan TD06414, Indianapolis, IN, USA) and tap water *ad libitum* for 10 weeks. Food was freely available, except when fasted prior to the glucose and insulin tolerance tests (ITTs). Body weight and calorie intake were measured once each week during the experimental periods. TM5441 was synthesized by Dr Toshio Miyata, and its characteristics and specificity were as described previously (Boe *et al.*, 2013). TM5441 was

administered daily with the initiation of HFD at a dose of 20 mg·kg⁻¹ by oral gavage. The ND and HFD groups were administered in an equal volume of 0.25% carboxymethyl cellulose by oral gavage. All animal experiments were approved by the Institutional Animal Care and Use Committee at Ewha Womans University (no. 2011-01-079).

In vivo insulin stimulation

For *in vivo* insulin stimulation and analysis of insulin signaling in adipose tissue, mice were fasted overnight, anaesthetized and then injected via the inferior vena cava with Humulin® (10 U·kg⁻¹, Eli Lilly, Indianapolis, IN, USA). Epididymal white adipose tissue (WAT) from the left side was removed 4 min after insulin injection as described previously (Jiang *et al.*, 2011).

Glucose tolerance test and ITT

The glucose tolerance test (GTT) was performed in mice after 16 h of food deprivation by orally administering 2.0 g glucose kg⁻¹ body weight (Pfluger *et al.*, 2008). Blood samples were taken from the tail vein to measure blood glucose levels before and 15, 30, 60, 90 and 120 min after glucose administration. The ITT was conducted after 6 h of food deprivation followed by an i.p. injection of 0.75 U·kg⁻¹ body weight Humulin (Eli Lilly). Blood glucose was measured using an ACCU-Check glucose meter (Roche Diagnostics, Laval, QC, Canada).

Morphometric and immunohistochemical analysis

Epididymal adipose tissues were fixed in 4% formalin, dehydrated and embedded in paraffin. Five micron sections were used for haematoxylin and eosin (H&E) staining. Digital images were captured with a Zeiss microscope equipped with an Axio Cam HRC digital camera and Axio Cam software (CarlZeiss, Thornwood, NY, USA), and a cell area of at least 500 adipocytes was measured with the open-source image analysis programme ImageJ v1.34s (Rasband, WS, ImageJ,

US National Institutes of Health, Bethesda, MD, <http://rsb.info.nih.gov/ij/>, 1997–2006).

Immunohistochemistry was performed using immunoperoxidase procedures and a commercially available kit (Dako, Glostrup, Denmark). The tissue sections were deparaffinized, and endogenous peroxidase was quenched with peroxidase solution (Dako) for 30 min. The sections were then washed and incubated with serum-free blocking solution (Dako), followed by incubation with anti-F4/80 (1:200, Santa Cruz Biotechnology Inc., Santa Cruz, CA, USA) overnight at 4°C. After being washed in PBS, sections were incubated with an LSAB2 kit (Dako) before exposure to 3, 3'-diaminobenzidine for 1 min. Images were photographed as described for the morphometric analysis.

Measurement of blood parameters and ELISA

Blood was centrifuged at 900 g for 15 min at 4°C, and the serum in the supernatant was collected. Fasted plasma triglyceride (TG), glycerol, free fatty acid (FFA) and total cholesterol were measured using an EnzyChrom™ colorimetric assay kit (BioAssay Systems, Hayward, CA, USA). For fasted plasma PAI-1 and insulin measurements, commercial ELISA kits (R&D Systems) were used according to the manufacturer's instruction.

Real-time quantitative reverse transcription PCR

The expression of mRNAs was assessed by real-time quantitative reverse transcription PCR using a SYBR Green PCR Master Mix kit (Applied Biosystems, Foster City, CA, USA) with an ABI 7300 real-time PCR thermal cycler (Applied Biosystems). The mRNA expression levels of the test genes were normalized to 18S rRNA levels. The primer sequences are listed in Table 1.

Western blot analysis

Adipose tissues were lysed and centrifuged at 16 000 g at 4°C for 15 min. The concentration of protein was determined using the Bradford methods (Bio-Rad Laboratories, Hercules, CA, USA), and aliquots of tissue homogenates were mixed

Table 1

Primer sequences

Gene name	Forward	Reverse
ATGL	5'-CTCATTGCTGGCTGCGGCT-3'	5'-CCCCAGTGACCAGCGCTGTG-3'
Cox4	5'-TCGATCGTACTGGGTGGCCA-3'	5'-GCCGAGGGAGTGAGGGAGGC-3'
Crif1	5'-CGCAATGCGGAGTGGCTAT-3'	5'-CGACTCTTGCATGGTCGCTA-3'
FAS	5'-CCTGGATAGCATTCCGAACCT-3'	5'-GCACATCTCGAAGGCTACACA-3'
HSL	5'-TGGGGAGCTCCAGTCGGAAGA-3'	5'-CATTAGACAGCCCGCGTGTG-3'
iNOS	5'-GGCAGCCTGTGAGACCTTTG-3'	5'-CATTGGAAGTGAAGCGTTTCG-3'
MCP-1	5'-CTTCTGGGCTGCTGTTC-3'	5'-CCAGCCTACTCATTGGGATCA-3'
mtDNA	5'-CCACTTCATCTTACCATTTA-3'	5'-ATCTGCATCTGAGTTTAATC-3'
PAI-1	5'-AGGGCTTCATGCCCCACTTCTTCA-3'	5'-AGTAGAGGGCATTACCAGCACCA-3'
PGC1 α	5'-TCGATGTGTCGCTTCTTGC-3'	5'-ACGAGAGCGCATCCTTTGG-3'
Tfam	5'-CGTGAGACGAACCGACGGC-3'	5'-GCACATCTCGACCCCGTGC-3'
UCP-1	5'-ACGTCCCCTGCCATTTACTG-3'	5'-CCCTTTGAAAAGGCCGTCG-3'

with sample buffer containing SDS and β -mercaptoethanol and heated at 95°C for 5 min. The samples were then applied to an SDS-PAGE gel and separated by electrophoresis. The proteins were transferred onto a PVDF membrane (GE Healthcare BioSciences Co., Piscataway, NJ, USA) in a transblot chamber with Tris buffer. The membrane was blocked for 1 h at room temperature with 5% skimmed milk in TBS-Tween 20 buffer, followed by an overnight incubation at 4°C in a 1:1000 dilution of the indicated antibodies. The following primary antibodies were purchased from Cell Signaling Technology (Danvers, MA, USA): anti-phospho-Akt (Ser⁴⁷³), anti-Akt, anti-phospho-hormone-sensitive lipase (HSL) (Ser⁵⁶³), anti-HSL antibody, adipose triglyceride lipase (ATGL) antibody, anti-phospho-JNK (Thr¹⁸³/Tyr¹⁸⁵) and anti-JNK. Anti-PAI-1 and anti- β -tubulin were purchased from Santa Cruz Biotechnology (Santa Cruz, CA, USA), anti-uncoupling protein (ucp)-1 was purchased from Abcam (Cambridge, MA, USA) and anti- β -actin was purchased from Sigma-Aldrich (St Louis, MO, USA) for immunoblotting. The membrane was then washed and incubated with peroxidase-conjugated secondary antibody for 1 h at room temperature. The washes were repeated, and the membrane was developed with an enhanced chemiluminescence detection reagent (GE Healthcare BioSciences Co.) according to the manufacturer's instructions. Positive immunoreactive bands were quantified using a densitometer (LAS-3000, FUJIFILM Corporation, Tokyo, Japan), normalized by β -tubulin, and compared with each control.

Statistical analysis

The data and statistical analysis comply with the recommendations on experimental design and analysis in pharmacology (Curtis *et al.*, 2015).

All results are expressed as the mean \pm SEM. ANOVA was used to assess differences between multiple groups. A *P* value < 0.05 was considered significant.

Results

TM5441 prevents HFD-induced obesity and systemic insulin resistance in mice

To generate a diet-induced obesity model, 10-week-old mice were placed on an HFD containing 60% calories from fat for 10 weeks. Rapid increase of body weight was observed from 4 weeks after the initiation of HFD compared with ND containing 18% calories from fat (Figure 1A). The weight gain was manifested by increased accumulation of both subcutaneous and epididymal fats. Absolute epididymal fat and subcutaneous fat from HFD mice weighted fivefold and eightfold more, respectively, than that of ND mice (Figure 1B). This change was consistent when corrected by body weight (Figure 1C). TM5441 significantly inhibited the HFD-induced increase in body weight and fat mass (Figure 1B, C). Calorie intake was not modified by TM5441 treatment: calorie intake in HFD and TM5441-treated HFD mice was 13.4 ± 0.7 and 12.6 ± 1.0 kcal day⁻¹ respectively. HFD mice exhibited enlarged adipocytes compared with ND mice, and TM5441

effectively reduced the adipocyte size, as shown by H&E staining (Figure 1D). The increased mean adipocyte size in HFD mice was consistently reduced in mice administered TM5441 (Figure 1E).

Administration of TM5441 significantly suppressed HFD-induced plasma TG and glycerol (Table 2). Although plasma FFA levels did not differ between the ND and HFD groups, TM5441 significantly reduced the plasma FFA concentration up to 30% compared with HFD mice (*P* < 0.05). Increased levels of LDL cholesterol in HFD mice were suppressed by TM5441 administration, although little change was observed in total and HDL cholesterol levels (Table 2).

HFD mice also exhibited glucose intolerance determined by GTT, and TM5441-administered HFD mice presented a trend of lowered blood glucose levels during the test (Figure 1F, H). ITT in HFD mice showed that TM5441 administration ameliorated glucose level in response to insulin from 30 to 120 min after injection (Figure 1G, I). In parallel, HbA_{1c} levels in the TM5441-administered HFD mice were decreased, when compared with HFD group. The high levels of fed and fast plasma insulin in HFD mice were decreased by 44% and 26%, respectively, by TM5441 administration. Results from GTT, ITT and fasting insulin levels suggest that TM5441 treatment may improve HFD-induced insulin resistance (Table 2).

TM5441 prevents HFD-induced dysregulation of lipid metabolism

HSL and ATGL protein levels were determined in the epididymal WAT to assess lipolysis in adipose tissue. HFD mice exhibited a significant reduction in phosphorylation of HSL (Ser⁵⁶³) and ATGL, suggesting a low lipolysis level, followed by excess TG storage in the WAT. TM5441 pretreatment prevented the decrease in HSL phosphorylation and ATGL (Figure 2A, B). These results are consistent with expansion of adipocyte size in HFD mice, which was reduced by TM5441 treatment (Figure 1D, E). Although HSL mRNA expression tended to be lower in HFD mice and was minimally altered after TM5441 treatment (Figure 2C), ATGL mRNA levels were significantly reduced up to 30% by the HFD and restored in TM5441-treated mice (Figure 2D). Fatty acid synthase (FAS), a lipogenic enzyme in epididymal WAT, was increased 3.5-fold by the HFD, in contrast to HSL and ATGL, and was significantly suppressed by TM5441 pretreatment (Figure 2E).

TM5441 prevents insulin resistance in the epididymal WAT of HFD mice

We then measured Akt Ser⁴⁷³ phosphorylation in epididymal WAT homogenates to determine the effect of TM5441 on HFD-induced insulin resistance. Western blot analysis indicated that insulin stimulation *in vivo* increased phosphorylated Akt approximately 5.5-fold. HFD mice exhibited a significant reduction in insulin-induced Akt activation, which was effectively restored by TM5441 (Figure 3A). We further investigated the phosphorylation of JNK (Thr¹⁸³/Tyr¹⁸⁵), because activation of JNK has been shown to cause insulin resistance in adipocytes (Hirosumi *et al.*, 2002). Western blotting of HFD adipose tissue lysates revealed a 2.0-fold increased JNK activation compared with ND mice;

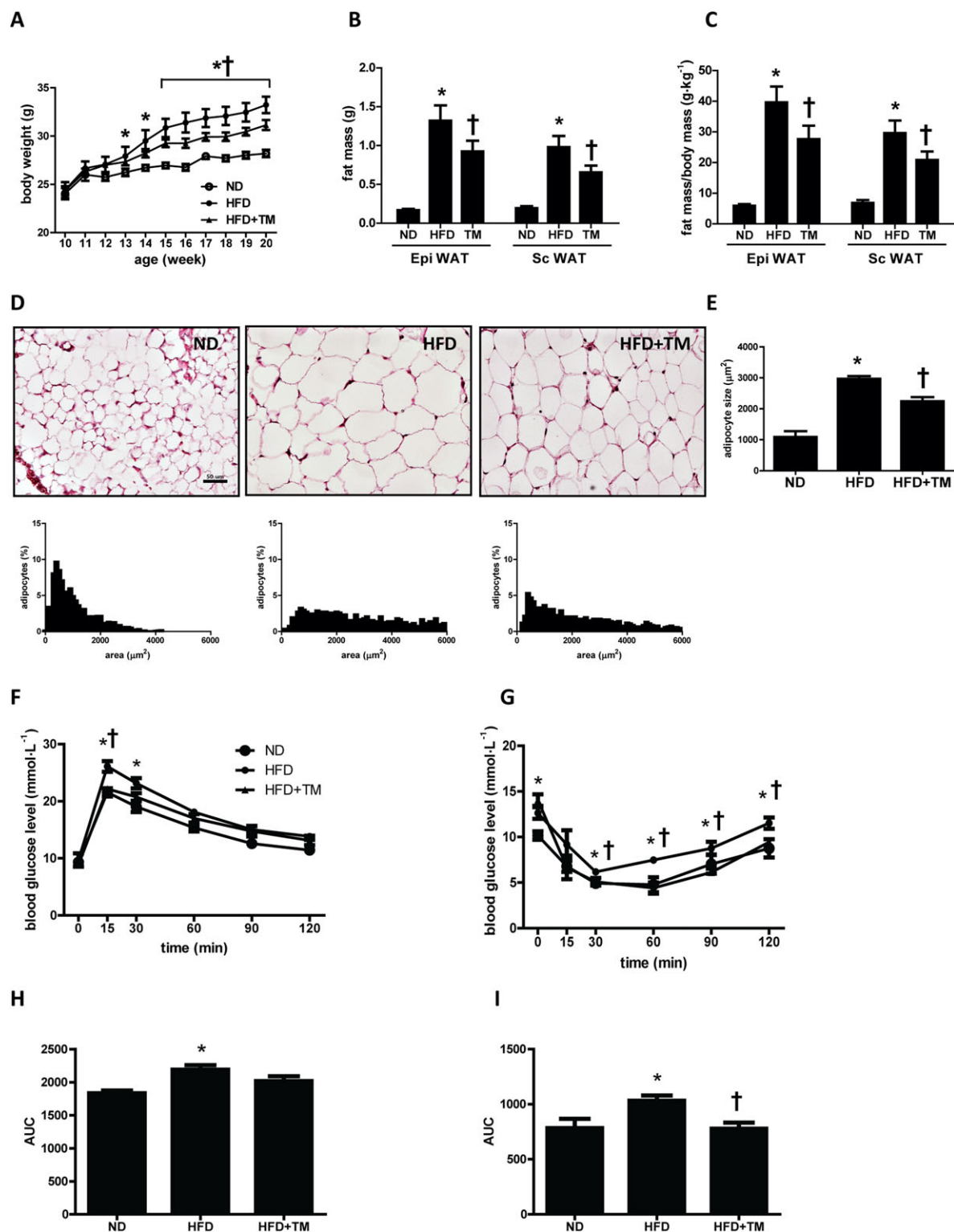


Figure 1

TM5441 prevents HFD-induced obesity and insulin resistance in mice. Ten-week-old C57BL/6J mice were fed ND, HFD or HFD plus TM5441 for 10 weeks. (A) Time course of body weight during the experimental period. (B and C) The fat mass and the fat weight/body weight ratio in epididymal WAT and subcutaneous WAT were measured before the animals were killed. (D and E) Histological analysis of epididymal WAT was conducted, and mean adipocyte size was measured. Representative H&E staining and distribution of adipocyte size in the epididymal WAT. For quantification, three mice were randomly selected from each group. Magnification, 200×; scale bar, 50 μm. (F) Blood glucose levels were during oral GTT at 8 weeks after HFD. (G) ITT was performed after 9 weeks on the HFD. (H and I) AUC for GTT and ITT was calculated using the trapezoidal method. The data are shown as the mean ± SEM of seven mice. * $P < 0.05$ versus ND, † $P < 0.05$ versus HFD.

Table 2

Metabolic parameters after 10 weeks of HFD

Plasma	ND	HFD	HFD + TM
Fed insulin (ng·mL ⁻¹)	0.49 ± 0.15	2.71 ± 0.41 ***	1.51 ± 0.18 * †
Fasting insulin (ng·mL ⁻¹)	0.57 ± 0.05	0.87 ± 0.13 *	0.64 ± 0.05
HbA _{1c} (%)	4.35 ± 0.02	4.60 ± 0.06 *	4.32 ± 0.10 †
Glycerol (mM)	0.32 ± 0.02	0.44 ± 0.05 *	0.32 ± 0.03 †
FFA (mM)	0.91 ± 0.08	0.88 ± 0.11	0.57 ± 0.08 * †
TG (mM)	0.46 ± 0.04	0.78 ± 0.10 *	0.59 ± 0.05 †
TC (mM)	1.89 ± 0.20	3.35 ± 0.21 *	3.08 ± 0.08 *
LDL (mM)	0.06 ± 0.03	0.31 ± 0.07 *	0.08 ± 0.07 †
HDL (mM)	1.25 ± 0.08	2.03 ± 0.23 *	1.89 ± 0.10 *
PAI-1 (ng·mL ⁻¹)	15.81 ± 5.40	45.00 ± 15.11 *	19.67 ± 3.33 †

Data are shown as mean ± SEM of seven mice.

P* < 0.05 versus ND.**P* < 0.001 versus ND.†*P* < 0.05 versus HFD.

TC, total cholesterol.

JNK activation was normalized to control levels in the adipose tissues of TM5441-treated HFD mice (Figure 3B).

TM5441 reduces inflammation in the epididymal WAT of HFD mice

To assess the effect of TM5441 on epididymal WAT inflammation, macrophage infiltration was measured. F4/80 immunohistochemistry staining in epididymal WAT to assess macrophage infiltration revealed an enhanced staining area and a crown-like structure around necrotic adipocytes in HFD mice, which was significantly reduced in WAT of TM5441-administered HFD mice (Figures 4A, B). Consistently, monocyte chemoattractant protein-1 (MCP-1) and inducible nitric oxide synthase (iNOS) mRNA expression were increased in HFD mice and reduced after TM5441 administration, although statistical significance was not reached for MCP-1 mRNA expression (Figures 4C, D). Western blotting of epididymal WAT homogenates demonstrated that HFD up-regulated PAI-1 protein expression, and TM5441 effectively inhibited HFD-induced PAI-1 protein up-regulation (Figure 4E). PAI-1 mRNA was 4.8-fold higher in the HFD group and was significantly reduced by TM5441 administration, consistent with the protein levels (Figure 4F). In addition, HFD mice exhibited higher plasma PAI-1 levels compared with ND mice, which was significantly reduced by TM5441.

TM5441 prevents mitochondrial dysfunction in the epididymal WAT of HFD mice

Mitochondrial dysfunction has been reported to cause adipose tissue dysfunction in both obesity and lipodystrophy (De Pauw *et al.*, 2009). To determine whether the protective effect of TM5441 on HFD-induced WAT inflammation and insulin resistance may be due to mitochondrial fitness, we analysed markers of mitochondrial biogenesis in WAT. PPAR γ coactivator-1 α (PGC1 α), mitochondrial transcription factor A (Tfam), cytochrome c oxidase 4 (Cox4) and mitochondrial DNA (mtDNA) mRNA levels were significantly reduced in

HFD mice compared with each of the ND mice, and these reductions were effectively prevented by TM5441 (Figures 5A–D). Crif1, the key regulator of mitochondrial oxidative phosphorylation, was also reduced in WAT of HFD mice and restored by TM5441 (Figure 5E). TM5441 significantly increased UCP-1 mRNA and protein expression in WAT of HFD mice (Figure 5F, G). Altogether, these data suggest that TM5441 improves metabolic stress-induced mitochondrial dysfunction in WAT.

Discussion

The present study provides experimental evidence that TM5441, a synthetic PAI-1 inhibitor (Boe *et al.*, 2013; Eren *et al.*, 2014; Placencio *et al.*, 2015), may become a novel therapeutic agent for obesity and obesity-related metabolic diseases. Administration of TM5441 effectively prevented HFD-induced obesity, which is consistent with previous studies in HFD-fed PAI-1 KO male mice (Schafer *et al.*, 2001; Ma *et al.*, 2004). Furthermore, a TM-series of PAI-1 inhibitors have been shown not to have an anti-obesity effect on HFD-fed PAI-1 KO mice (personal communication from Dr T. Miyata), supporting the notion that the anti-obesity effects of TM5441 are PAI-1-dependent. However, in a previous study it was demonstrated that PAI-1 deficiency improved obesity-related metabolic disorders without affecting adiposity in female mice (Tamura *et al.*, 2014), and PAI-1 deficiency did not affect the body weight in streptozotocin-induced type 1 diabetic female mice (Mao *et al.*, 2014). While the exact reason for this difference is not clear, differences in genetic background, animal sex and high-fat food formula possibly account for the different outcomes. For example, C57BL/6 mice are sensitive to diet-induced obesity and hepatosteatosis, but A/J mice are resistant (Hall *et al.*, 2010). In this connection, Schafer *et al.* (2001) and Ma *et al.* (2004) used PAI-1 deficient mice with C57BL/6

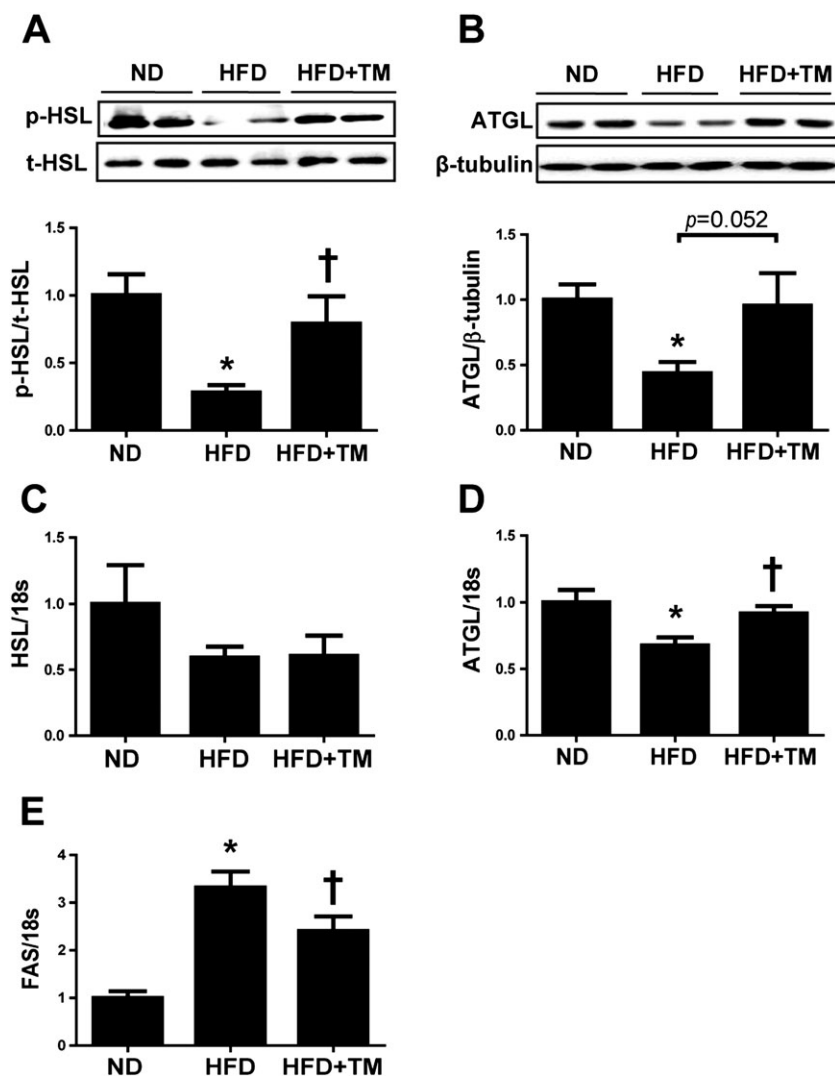


Figure 2

TM5441 normalizes the alterations in lipid metabolism-related enzymes induced by a HFD. (A and B) Western blotting analysis of HSL and ATGL in epididymal WAT lysates. (C–E) Total RNA was isolated from the epididymal WATs and subjected to quantitative reverse transcription PCR analysis to determine the expression of (C) HSL, (D) ATGL and (E) FAS. Expression was normalized against 18S rRNA levels. The data are shown as the mean \pm SEM of seven mice. * $P < 0.05$ versus ND, † $P < 0.05$ versus HFD.

genetic background, but Tamura *et al.* (2014) and Mao *et al.* (2014) used mixed genetic background.

HFD-induced adipocyte hypertrophy, down-regulation of HSL phosphorylation and ATGL expression and up-regulation of FAS expression were prevented by TM5441 treatment. These data imply that large adipocytes in HFD mice accumulate cytosolic lipids by decreasing lipolysis and increasing lipogenesis through PAI-1. Decreased plasma FFA and glycerol at the presence of increased lipolysis in TM5441-treated HFD mice WAT suggest that other tissues such as liver and brown adipose tissue may take up. Conflicting data on HSL and ATGL changes in the WAT of obese mice have been reported. Decreased HSL phosphorylation but increased ATGL levels were reported in mice fed a HFD for 8-weeks (Gaidhu *et al.*, 2010). Another study demonstrated enhanced basal lipolysis, accompanied by increased HSL and ATGL mRNA expression, in large adipocytes isolated

from mice fed a HFD for 8 weeks (Wueest *et al.*, 2009). Differences in the mouse model and experimental conditions may account for these different observations.

It is commonly recognized that weight gain results from an imbalance between energy intake and expenditure. The effect of TM5441 on adiposity does not appear to be decreased caloric intake; calorie intake in HFD and TM5441-treated HFD mice was 13.41 ± 0.67 and 12.62 ± 1.02 kcal day⁻¹, respectively, in the present study. In contrast, reversal of HFD-induced PGC1 α , Tfam, mtDNA, Crif1 and Ucp-1 down-regulation suggests that TM5441 induces mitochondrial biogenesis and mitochondria metabolism under HFD. PAI-1 deficient mice on an HFD exhibited increased energy expenditure along with UCP-3 up-regulation in skeletal muscle compared with wild type mice (Ma *et al.*, 2004).

Consistent with the results of HFD-fed PAI-1 KO mice (Ma *et al.*, 2004), TM5441 prevented systemic glucose and insulin

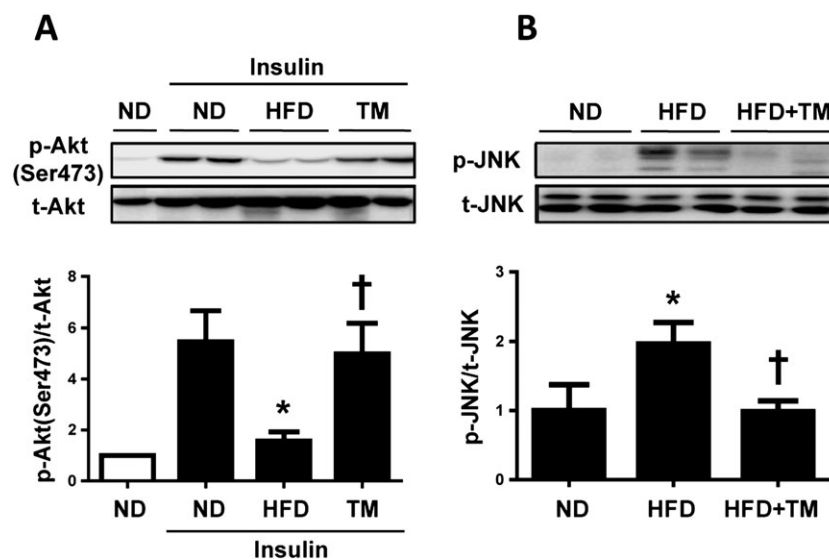


Figure 3

TM5441 enhances insulin signalling and suppresses JNK phosphorylation in the epididymal WAT of HFD mice. (A) Insulin-stimulated phosphorylation of Akt (Ser⁴⁷³) in the epididymal WAT was determined by western blot analysis. The three groups of mice were fasted overnight, before injection with insulin, and the epididymal WAT was removed 4 min after insulin injection. (B) Phosphorylation of JNK in the epididymal WAT was determined by western blot analysis. The data were shown as representative western blots and the mean \pm SEM of seven mice. * $P < 0.05$ versus ND, † $P < 0.05$ versus HFD.

intolerance and high plasma insulin levels in HFD mice. In the present study, the decreased phosphorylation of Akt in epididymal WAT of mice fed an HFD compared with those fed an ND was restored by TM5441 treatment, suggesting that

PAI-1 plays an important role in dysregulating insulin signalling in WAT. Although adipose tissue insulin resistance is the prominent feature of diet-induced obesity (Olefsky and Glass, 2010), it is still important to investigate whether the TM5441

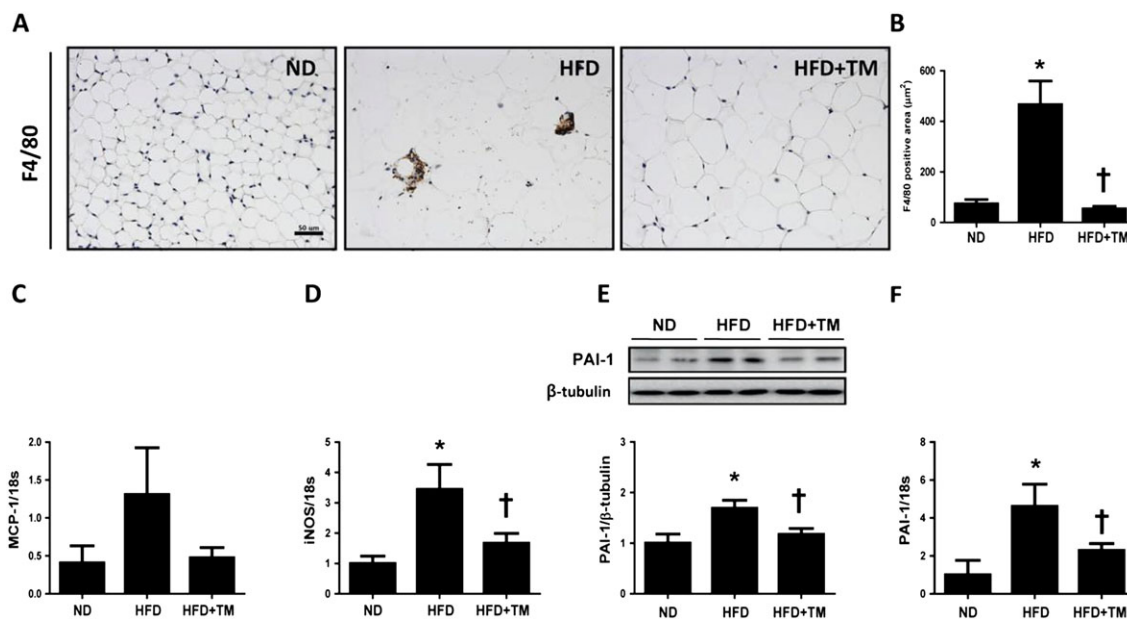


Figure 4

TM5441 prevents HFD-induced inflammation in the epididymal WAT. (A and B) Representative immunohistochemical staining of F4/80 (1:200) and quantification of F4/80-positive area in epididymal WAT. Magnification, 100 \times ; scale bar, 100 μm . (C and D) MCP-1 and iNOS mRNA levels were determined by quantitative reverse transcription PCR (qRT-PCR). (E and F) PAI-1 protein and mRNA expression in the epididymal WAT were determined by western blot analysis and qRT-PCR. The data are shown as the mean \pm SEM of seven mice. * $P < 0.05$ versus ND, † $P < 0.05$ versus HFD.

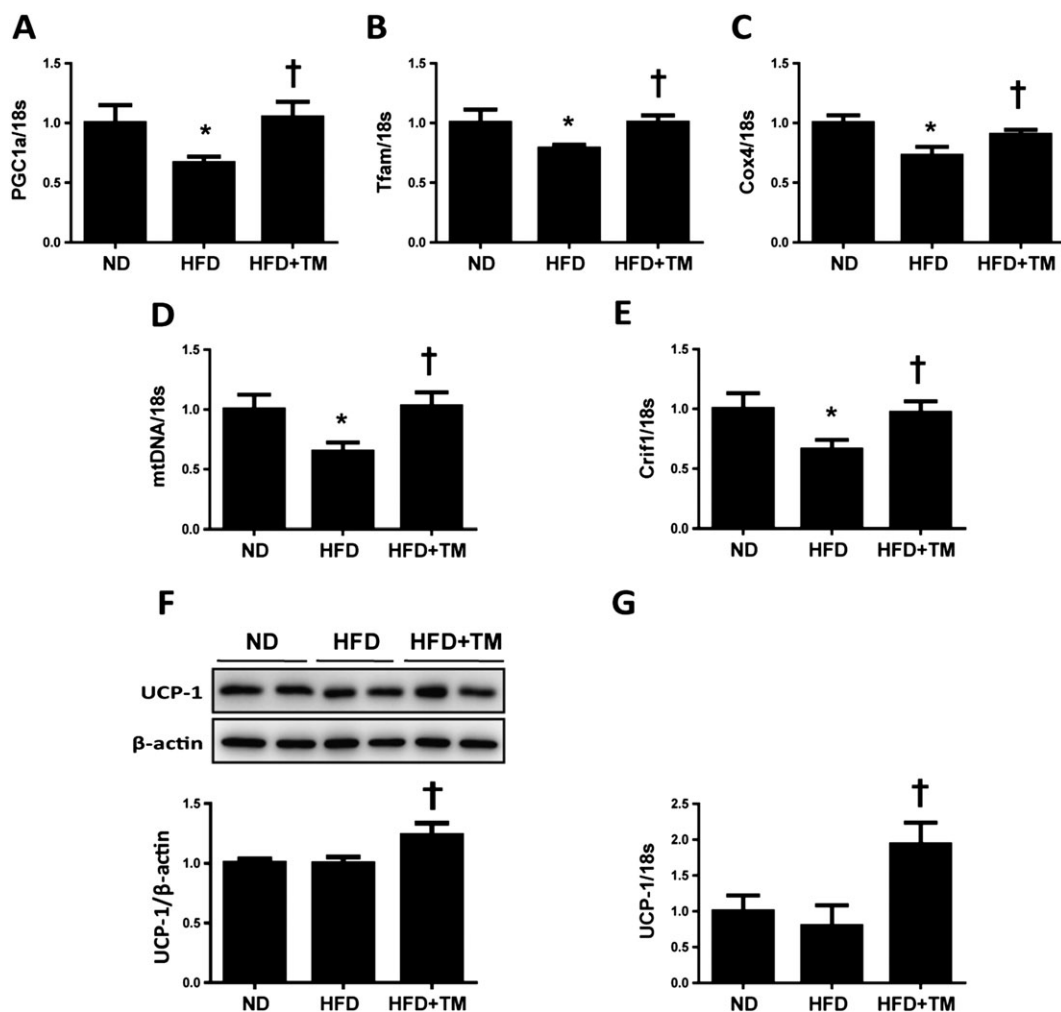


Figure 5

TM5441 restores HFD-induced mitochondrial dysfunction in the epididymal WAT. (A–E) Total RNA was isolated from the epididymal WATs and subjected to quantitative reverse transcription PCR analysis to determine the expression of (A) PGC1 α , (B) Tfam, (C) Cox4, (D) mtDNA, (E) Crif1 and (G) UCP-1. Expression was normalized against 18S rRNA levels. (F) UCP-1 protein expression level was detected by western blot analysis, where β -actin was used as an internal control. The data are shown as the mean \pm SEM of seven mice. * $P < 0.05$ versus ND, † $P < 0.05$ versus HFD.

has beneficial effects in other tissues such as liver and skeletal muscle. A recent study by Tamura *et al.* (2015) showed PAI-1 induces insulin resistance in hepatocytes.

Chronic inflammation accompanied by adipose tissue macrophage infiltration is the major feature of obesity (Gregor and Hotamisligil, 2011). HFD-induced MCP-1 and iNOS mRNA up-regulation in WAT were also effectively inhibited by TM5441 treatment, suggesting less macrophage recruitment to the adipose tissue. This was confirmed by immunostaining of epididymal WAT, which revealed that the mature macrophage marker F4/80 was decreased in TM5441-treated mice. Adipokine dysregulation, as represented by adiponectin down-regulation and PAI-1 up-regulation, is another feature in the WAT of obese mice (Maury and Brichard, 2010). While adiponectin mRNA and protein in WAT of HFD mice were not decreased in the present study (data not shown), PAI-1 mRNA and protein expression were increased in WAT of HFD mice. TM5441 effectively inhibited HFD-induced PAI-1 up-regulation. This

decreased PAI-1 expression in response to the PAI-1 inhibitor, TM5441, can be postulated as follows: TM5441 inhibits PAI-1-induced adipocytes dysfunction in HFD mice, allowing them to function as normal adipocytes with respect to PAI-1 expression. Significant suppression of PAI-1 mRNAs in experimental animals given PAI-1 inhibitors has been demonstrated previously in various disease models, such as the NEP25/LMB2 podocyte injury mouse model (Kobayashi *et al.*, 2015) and anti-Thy-1 rat glomerulonephritis model (Ichimura *et al.*, 2013), as well as in the rodent multiple sclerosis models (Pelisch *et al.*, 2015), and bleomycin-injured lung fibrosis (Omori *et al.*, 2016). These results suggest the positive feedback loop between PAI-1 activity and expression.

While the mechanisms by which TM5441 prevents inflammation in adipocytes have not been clearly elucidated, mitochondrial fitness is essential for adipocyte homeostasis (Rong *et al.*, 2007; Wang *et al.*, 2013). A recent study using adipose-specific Crif1 deficient mice further suggests that impaired mitochondrial oxidative phosphorylation in WAT

determines its metabolic and inflammatory response and causes systemic insulin resistance (Ryu *et al.*, 2013). In our study, mRNA expression of Crif1, UCP-1 and mitochondrial biogenesis markers (PGC1 α , Tfam, Cox4 and mtDNA) were all decreased in WAT of HFD mice, which was prevented by TM5441. These data suggest that PAI-1 may induce dysregulation of mitochondrial fitness in WAT. The exact pathways how PAI-1 regulates mitochondrial fitness remain to be studied. Considering the emerging concept that fibrosis is a major player in adipose tissue dysfunction (Sun *et al.*, 2013) and that PAI-1 is implicated in the development and progression of tissue fibrosis (Ghosh and Vaughan, 2012), the role of PAI-1 in HFD-induced adipose tissue fibrosis also remains to be studied.

The significance and novelty of the present study is that it provides experimental data that a newly developed orally active PAI-1 inhibitor, TM5441, protects against progressive obesity and obesity-related adipocyte dysfunction by enhancing mitochondrial fitness.

Acknowledgements

This work was financially supported by NLRL through the National Research Foundation (NRF) of Korea (no. 2012R1A2A1A0300692). We are grateful to Jung Hwa Lee for her excellent technical assistance.

Author contributions

L.P., I.J., J.Y.H. and H.H. conceived and designed the experiments. L.P. and I.J. contributed to perform the experiments and analysed data. T.M. synthesized TM5441. L.P., I.J. and H.H. contributed to the writing of the manuscript. H.H. approved the final version to be published.

Conflict of interest

The authors declare no conflicts of interest.

Declaration of transparency and scientific rigour

This Declaration acknowledges that this paper adheres to the principles for transparent reporting and scientific rigour of preclinical research recommended by funding agencies, publishers and other organisations engaged with supporting research.

References

Alexander SPH, Fabbro D, Kelly E, Marrion N, Peters JA, Benson HE *et al.* (2015a). The concise guide to PHARMACOLOGY 2015/16: enzymes. *Br J Pharmacol* 172: 6024–6109.

Alexander SPH, Kelly E, Marrion N, Peters JA, Benson HE, Faccenda E *et al.* (2015b). The concise guide to PHARMACOLOGY 2015/16: transporters. *Br J Pharmacol* 172: 6110–6202.

Boe AE, Eren M, Murphy SB, Kamide CE, Ichimura A, Terry D *et al.* (2013). Plasminogen activator inhibitor-1 antagonist TM5441 attenuates Nomega-nitro-L-arginine methyl ester-induced hypertension and vascular senescence. *Circulation* 128: 2318–2324.

Crandall DL, Quinet EM, Ayachi S, Hreha AL, Leik CE, Savio DA *et al.* (2006). Modulation of adipose tissue development by pharmacological inhibition of PAI-1. *Arterioscler Thromb Vasc Biol* 26: 2209–2215.

Curtis MJ, Bond RA, Spina D, Ahluwalia A, Alexander SP, Giembycz MA *et al.* (2015). Experimental design and analysis and their reporting: new guidance for publication in BJP. *Br J Pharmacol* 172: 3461–3471.

De Pauw A, Tejerina S, Raes M, Keijer J, Arnould T (2009). Mitochondrial (dys)function in adipocyte (de)differentiation and systemic metabolic alterations. *Am J Pathol* 175: 927–939.

Eren M, Boe AE, Murphy SB, Place AT, Nagpal V, Morales-Nebreda L *et al.* (2014). PAI-1-regulated extracellular proteolysis governs senescence and survival in Klotho mice. *Proc Natl Acad Sci U S A* 111: 7090–7095.

Gaidhu MP, Anthony NM, Patel P, Hawke TJ, Ceddia RB (2010). Dysregulation of lipolysis and lipid metabolism in visceral and subcutaneous adipocytes by high-fat diet: role of ATGL, HSL, and AMPK. *Am J Physiol Cell Physiol* 298: 961–971.

Ghosh AK, Vaughan DE (2012). PAI-1 in tissue fibrosis. *J Cell Physiol* 127: 493–507.

Gorlatova NV, Cale JM, Elokda H, Li D, Fan K, Warnock M *et al.* (2007). Mechanism of inactivation of plasminogen activator inhibitor-1 by a small molecule inhibitor. *J Biol Chem* 282: 9288–9296.

Gregor MF, Hotamisligil GS (2011). Inflammatory mechanisms in obesity. *Annu Rev Immunol* 29: 415–445.

Hall D, Poussin C, Velagapudi VR, Empsen C, Joffraud M, Beckmann JS *et al.* (2010). Peroxisomal and microsomal lipid pathways associated with resistance to hepatic steatosis and reduced pro-inflammatory state. *J Biol Chem* 285: 31011–31023.

Hirosumi J, Tuncman G, Chang L, Gorgun CZ, Uysal KT, Maeda K *et al.* (2002). A central role for JNK in obesity and insulin resistance. *Nature* 420: 333–336.

Hotamisligil GS (2006). Inflammation and metabolic disorders. *Nature* 444: 860–867.

Huh JY, Kim Y, Jeong J, Park J, Kim I, Huh KH *et al.* (2012). Peroxiredoxin 3 is a key molecule regulating adipocyte oxidative stress, mitochondrial biogenesis, and adipokine expression. *Antioxid Redox Signal* 16: 229–243.

Ichimura A, Matsumoto S, Suzuki S, Dan T, Yamaki S, Sato Y *et al.* (2013). A small molecule inhibitor to plasminogen activator inhibitor 1 inhibits macrophage migration. *Arterioscler Thromb Vasc Biol* 33: 935–942.

Izuhara Y, Yamaoka N, Kodama H, Dan T, Takizawa S, Hirayama N *et al.* (2010). A novel inhibitor of plasminogen activator inhibitor-1 provides antithrombotic benefits devoid of bleeding effect in nonhuman primates. *J Cereb Blood Flow Metab* 30: 904–912.

Jiang C, Qu A, Matsubara T, Chanturiya T, Jou W, Gavrilova O *et al.* (2011). Disruption of hypoxia-inducible factor 1 in adipocytes improves insulin sensitivity and decreases adiposity in high-fat diet-fed mice. *Diabetes* 60: 2484–2495.

- Juhan-Vague I, Alessi MC, Vague P (1991). Increased plasma plasminogen activator inhibitor 1 levels. A possible link between insulin resistance and atherothrombosis. *Diabetologia* 34: 457–462.
- Kilkenny C, Browne W, Cuthill IC, Emerson M, Altman DG (2010). Animal research: reporting *in vivo* experiments: the ARRIVE guidelines. *Br J Pharmacol* 160: 1577–1579.
- Kobayashi N, Ueno T, Ohashi K, Yamashita H, Takahashi Y, Sakamoto K *et al.* (2015). Podocyte injury-driven intracapillary plasminogen activator inhibitor type 1 accelerates podocyte loss via uPAR-mediated beta1-integrin endocytosis. *Am J Physiol Renal Physiol* 308: 614–626.
- Ma LJ, Mao SL, Taylor KL, Kanjanabuch T, Guan Y, Zhang *et al.* (2004). Prevention of obesity and insulin resistance in mice lacking plasminogen activator inhibitor 1. *Diabetes* 53: 336–346.
- Mao L, Kawao N, Tamura Y, Okumoto K, Okada K, Yano M *et al.* (2014). Plasminogen activator inhibitor-1 is involved in impaired bone repair associated with diabetes in female mice. *PLoS One* 9: e92686.
- Maury E, Brichard SM (2010). Adipokine dysregulation, adipose tissue inflammation and metabolic syndrome. *Mol Cell Endocrinol* 314: 1–16.
- McGrath JC, Lilley E (2015). Implementing guidelines on reporting research using animals (ARRIVE etc.): new requirements for publication in BJP. *Br J Pharmacol* 172: 3189–3193.
- Mertens I, Verrijken A, Michiels JJ, Van der Planken M, Ruige JB, Van Gaal LF (2006). Among inflammation and coagulation markers, PAI-1 is a true component of the metabolic syndrome. *Int J Obes (Lond)* 30: 1308–1314.
- Olefsky JM, Glass CK (2010). Macrophages, inflammation, and insulin resistance. *Annu Rev Physiol* 72: 219–246.
- Omori K, Hattori N, Senoo T, Takayama Y, Masuda T, Nakashima T *et al.* (2016). Inhibition of plasminogen activator inhibitor-1 attenuates transforming growth factor-beta-dependent epithelial mesenchymal transition and differentiation of fibroblasts to myofibroblasts. *PLoS One* 11: e0148969.
- Patti ME, Corvera S (2010). The role of mitochondria in the pathogenesis of type 2 diabetes. *Endocr Rev* 31: 364–395.
- Pelisch N, Dan T, Ichimura A, Sekiguchi H, Vaughan DE, van Ypersele de Strihou C *et al.* (2015). Plasminogen activator inhibitor-1 antagonist TM5484 attenuates demyelination and axonal degeneration in a mice model of multiple sclerosis. *PLoS One* 10: e0124510.
- Pfluger PT, Herranz D, Velasco-Miguel S, Serrano M, Tschop MH (2008). Sirt1 protects against high-fat diet-induced metabolic damage. *Proc Natl Acad Sci U S A* 105: 9793–9798.
- Placencio VR, Ichimura A, Miyata T, DeClerck YA (2015). Small molecule inhibitors of plasminogen activator inhibitor-1 elicit anti-tumorigenic and anti-angiogenic activity. *PLoS One* 10: e0133786.
- Rong JX, Qiu Y, Hansen MK, Zhu L, Zhang V, Xie M *et al.* (2007). Adipose mitochondrial biogenesis is suppressed in db/db and high-fat diet-fed mice and improved by rosiglitazone. *Diabetes* 56: 1751–1760.
- Rudich A, Kanety H, Bashan N (2007). Adipose stress-sensing kinases: linking obesity to malfunction. *Trends Endocrinol Metab* 18: 291–299.
- Ryu MJ, Kim SJ, Kim YK, Choi MJ, Tadi S, Lee MH *et al.* (2013). Crif1 deficiency reduces adipose OXPHOS capacity and triggers inflammation and insulin resistance in mice. *PLoS Genet* 9: e1003356.
- Schafer K, Fujisawa K, Konstantinides S, Loskutoff DJ (2001). Disruption of the plasminogen activator inhibitor-1 gene reduces the adiposity and improves the metabolic profile of genetically obese and diabetic ob/ob mice. *FASEB J* 15: 1840–1842.
- Smyth S, Heron A (2006). Diabetes and obesity: the twin epidemics. *Nat Med* 12: 75–80.
- Southan C, Sharman JL, Benson HE, Faccenda E, Pawson AJ, Alexander SP *et al.* (2016). The IUPHAR/BPS Guide to PHARMACOLOGY in 2016: towards curated quantitative interactions between 1300 protein targets and 6000 ligands. *Nucleic Acids Res* 44: D1054–D1068.
- Sun K, Tordjman J, Clement K, Scherer PE (2013). Fibrosis and adipose tissue dysfunction. *Cell Metab* 18: 470–477.
- Tamura Y, Kawao N, Yano M, Okada K, Matsuo O, Kaji H (2014). Plasminogen activator inhibitor-1 deficiency ameliorates insulin resistance and hyperlipidemia but not bone loss in obese female mice. *Endocrinology* 155: 1708–1717.
- Tamura Y, Kawao N, Yano M, Okada K, Okumoto K, Chiba *et al.* (2015). Role of plasminogen activator inhibitor-1 in glucocorticoid-induced diabetes and osteopenia in mice. *Diabetes* 64: 2194–2206.
- Wang CH, Wang CC, Huang HC, Wei YH (2013). Mitochondrial dysfunction leads to impairment of insulin sensitivity and adiponectin secretion in adipocytes. *FEBS J* 280: 1039–1050.
- Wuest S, Rapold RA, Rytka JM, Schoenle EJ, Konrad D (2009). Basal lipolysis, not the degree of insulin resistance, differentiates large from small isolated adipocytes in high-fat fed mice. *Diabetologia* 52: 541–546.